Land Contamination & Reclamation, 15 (4), 2007

DOI 10.2462/09670513.878

Ion exchange in birnessite

Lina Al-Attar and Alan Dyer

Abstract

Ion exchange isotherms for the sodium form of birnessite, a layered manganese oxide common in soils, were determined using isotope dilution analysis, by employing ^{22}Na to pre-label the solid. The results were represented by plotting the equivalent ionic fraction of an entering cation in the ion exchanger versus the equivalent ionic fraction of the entering cation remaining in solution. Studying these ion exchange isotherms for sodium-univalent (i.e. NH_4–Na, Li–Na, K–Na, and Cs–Na) and sodium-divalent pairs (Mg–Na, Ca–Na, Sr–Na and Ba–Na) on ^{22}Na-birnessite made it possible to obtain a clear picture of the exchangeable sites available in birnessite. The isotherms also gave an estimation of the effect of cations likely to be present in aqueous environments on the uptake of the fission product radioisotopes of caesium and strontium onto soils.

Key words: birnessite, cation exchange, manganese oxide, radioisotopes

1 INTRODUCTION

The presence of radioisotopes in the environment can arise from accidents, such as Chernobyl, and leakage from storage facilities at nuclear sites. In addition, the advised underground disposal of radioactive wastes is based upon multi-barrier concepts involving barrier and backfill materials (CoMRW 2006). Should containment be disrupted, knowledge of the possible interaction of radioisotopes with the 'far-field' is important (Bruno *et al*. 2004). Clearly the potential uptake of radioisotopes on to soils in the 'far-field' has a considerable impact in all these scenarios.

Birnessite was first reported in the Birness region of Scotland by Jones and Milne (1956). It is the main Mn-bearing phase in soils, and in marine manganese nodules and micro-nodules. It forms part of a family of porous manganese oxides with layered and tunnel structures. Most of the structural frameworks of these manganese oxides consist of manganese oxide $(MnO_6)^{8-}$ octahedral units shared by corners and/or edges. Because manganese oxides exhibit excellent ion exchange and molecule sorptive properties, they can be used as cation or molecular sieves (Feng *et al*. 1992; Shen *et al*. 1993).

Birnessite behaves as an ion-sieve material with an effective pore diameter of 3 Å, with a preference for the heavy metals, particularly cobalt, in soil and marine environments (McKenzie 1970; Golden *et al*. 1986*a*,1987).The structure of Na-birnessite consists of two-dimensional layers of edge-shared MnO_6 octahedra separated by exchangeable Na ions which reside in a single sheet of water molecules (Golden *et al*. 1987). The basal spacing of this mineral is *c*. 7.1 Å in the dry state. Na-birnessite results from the dehydration of buserite, which has a basal spacing of about 10 Å, and contains two-dimensional layers of edge-shared MnO_6 octahedra separated by double water molecule sheets holding Na^+ cations (Shen *et al*. 1994). Since Na^+ hydration is weak, the waters in Na-buserite (basal spacing *c*. 10 Å) are easily lost, transforming the buserite structure to birnessite (basal spacing *c*. 7.1 Å) after drying.

Previous work by these authors illustrated the supe-

Received February 2007; accepted July 2007

Authors
Lina Al-Attar and Alan Dyer*
Institute of Materials Research, Cockcroft Building, University of Salford, Salford M5 4WT, UK
*Corresponding author. Tel. +44 1254 761 384, email aldilp@aol.com

rior uptake behaviour of this material for uranium (Al-Attar and Dyer 2002) and other radioisotopes present in radioactive waste effluents (Dyer *et al*. 2000*a*,*b*; Al-Attar *et al*. 2003*a*,*b*) when it was compared to titanosilicates (Al-Attar *et al*. 2000, 2003*b*; Al-Attar and Dyer 2001) and antimony silicate (Al-Attar *et al*. 2004). The work here describes the construction of cation exchange isotherms for birnessite, using ^{22}Na-labelled birnessite in contact with selected cation solutions. Classical ion exchange theory enabled selectivity series to be constructed from estimated thermodynamic parameters derived from isotherm data. The series show the preferences that birnessite exhibits in its uptake of the fission-product cations strontium and caesium when they are in competition with other cations common in soils and environmental waters.

2 EXPERIMENTAL

2.1 Chemicals

The chemicals used in this work were of reagent grade, obtained from commercial suppliers, and used without further purification.

Radioactive sodium (^{22}Na) as sodium chloride carrier free was supplied by Amersham International Ltd., UK.

2.2 Preparation of ^{22}Na-birnessite for ion exchange studies

Birnessite was synthesized by oxidizing manganese chloride using oxygen in strongly basic conditions, as described by Golden *et al*. (1986*b*). A ^{22}Na-birnessite sample was then prepared by equilibrating the birnessite with 1 M ^{22}Na-spiked sodium nitrate solution for three days, after which it was air dried.

2.3 Characterization

An X-ray diffractogram of ^{22}Na-labelled birnessite was collected on a Siemens D5000 diffractometer with Cu-Kα radiation. Operating conditions were λ = 1.54179 Å, 2θ range 6–50, step size 0.02º, time 10 sec/step, T = 293 K, 40 mA current and a voltage of 40 V. Water contents of ^{22}Na-birnessite samples, pre-equilibrated in a desiccator over a saturated NaCl solution for two weeks, were determined by thermogravimetry (TGA) using a Mettler TA3000 system, at a heating rate of 5 K min^{-1}, under a nitrogen atmosphere.

2.4 Cation exchange experiments

Establishing a solution–solid equilibrium time was necessary to construct the isotherms. This was defined by running preliminary kinetic experiments for each of the in-going cations. A time of four hours was found to be adequate to achieve equilibrium between the two phases.

To carry out the forward isotherms of the cation pairs: NH_4–Na, Li–Na, K–Na, Rb–Na, Cs–Na, Mg–2Na, Ca–2Na, Sr–2Na and Ba–2Na, a set of eleven standard solutions for each competing ion was prepared. They contained a mixture of sodium and in-going cations in varying, but known, proportions, to attain a total normality (T_N) of 0.2 N. The anion present was always the nitrate ion.

For each individual cation, a series of eleven 20 mg tared ^{22}Na-birnessite samples, were placed in individual 15 mL polyethylene centrifuge vials and equilibrated with 4 mL of the appropriate 0.2 N solutions (V:M 200). The vials were capped, shaken and packed in a drum and rolled horizontally on a mineralogical roller at 298 K for a period of four hours. The vials were removed, and centrifuged using a Centaur MSE-2 (Orme) centrifuge for 15 min. at 4000 rpm. 2 mL of the supernatant solution was then withdrawn and filtered through a 0.2 μm PVDF membrane (Whatman). Radiochemical solution phase analyses were used to assess the extent of cation replacement, using isotope dilution analysis, by determining the activity of ^{22}Na in 1 mL of the filtrate using a pre-set protocol on a Canberra Packard 1900CA Tri-Carb liquid scintillation counter.

Reverse isotherms were constructed by adding 2 mL of the 100% sodium solution or 100% of the M-exchanging cation solution into the vials (which contained the solid material) together with the 2 mL left from each forward isotherm experiment. The vials were re-sealed, shaken and placed into a drum to roll for a further eight-hour equilibration period. The vials were removed, centrifuged and filtered, and the ^{22}Na activity of 1 mL of the filtrate was determined.

2.5 Isotherms

Binary cation exchange isotherms were plotted based upon the measured equivalent fractions of the in-going cation in solution (A_S) and solid (A_C) phases. They are illustrated in Figures 1 (a) to 8 (a), with plots of lnK_C versus A_C shown in Figures 1 (b) to 8 (b). K_C is the

Kielland coefficient, defined as follows:

$$K_C = A_C^{ZB} (m_B)_B^{ZA} \Gamma / B_C^{ZA} (m_A)_A^{ZB} \qquad (1.1)$$

where A_C^{ZB} and B_C^{ZA} are the equivalent fractions of ions A and B in the birnessite mineral, m_A and m_B are the concentrations of ions A and B in solutions (mol dm^{-3}), and Γ is the ratio of the corresponding single ion activity coefficients in solutions. Kielland plots were constructed using the Kielland program from the University of Salford network. This program made all the required corrections for the ionic activity coefficients of solid and solution phases, based on the methodology of Fletcher and Townsend (1982). Full details of these corrections can be found in a recent review by Dyer (2005). Standard free energies (ΔG^{θ}) for the exchange processes were generated by the same program.

3 RESULTS AND DISCUSSION

3.1 Birnessite characterization

Table 2 summarizes the chemical and physical characteristics of birnessite. The XRD pattern of birnessite (not shown) was identical to that given in previous literature (Golden *et al*. 1986*a*) and is indicative of a monoclinic one-layer structure with the interlayer *d*-spacing of *c*. 7 Å. Cation exchanged forms gave similar spacings with some exceptions that will be considered later.

Thermogravimetric analysis in the range 322–997 K showed a total mass loss of 20.49%, with two major peaks at 440 and 845 K. The first peak (mass loss 9.97%) represented the dehydration of sodium ions, located in between the two manganese oxide sheets, while the other peak can be ascribed to dehydroxylation.

Table 1. Birnessite ($Na_4Mn_{14}O_{27} \cdot 9H_2O$)

Theoretical CEC	3.15 meq g^{-1}
Diagnostic XRD peaks	7.20, 3.58, 2.52 Å
First mass loss (309–465 K)	9.97%

3.2 Ion exchange isotherms

It can be seen that there is a degree of experimental scatter in most isotherms. It is likely that the agitation of samples for four hours produces fine/colloidal particles which, despite careful centrifuge procedures, are carried over into the solution and so will affect the accurate determination of the solution activity. This is evident from the worsening of scatter seen in the reverse isotherms which have been agitated for eight hours. Scatter in the reverse arms can also arise from the difficulty in measuring the smaller amounts of radioactivity in these samples. Despite these difficulties, it is still possible to draw useful inferences from the isotherms with regard to the cation preferences shown by birnessite when it is in contact with more than one cation competing for exchange sites in the solid phase. When these include cations of the nuclear fission products strontium and caesium, assessment of the importance of birnessite as a soil component can be made.

Note that the A_C^{ZB} values have been calculated from the theoretical cation capacity given in Table 1. The fact that no 'over exchange' was observed confirms that the processes observed were those solely of movement of cations in the Mn octahedral layers. This means that there was no evidence of cation uptake involving the hydroxyl groups in the structure.

3.3 Uni-univalent exchanges

Figures 1(a) – 4(a) showed that all univalent cations, apart from Li, completely replaced the sodium ions initially present in ^{22}Na-birnessite, and exhibited different degrees of selectivity. Clearly, each of these cations, irrespective of its bare or hydrated radius, was capable of entering the interlayer system of birnessite. Full exchange suggested an absence of inaccessible sites, and that all the sodium ions were located between the octahedral manganese oxide layers. The lithium cation gave a sigmoidal isotherm, indicating an initial selectivity for the lithium cation, followed by a selectivity reversal with increasing equivalent fraction in the solid. The overall lack of selectivity for lithium over sodium can be attributed to the large hydration energy of lithium and the consequent difficulty in removing its co-ordinated water molecules. The other univalent cations, whose apparent hydrated sizes were larger than that of lithium but had lower hydration energies, could more easily shed their hydration sphere.

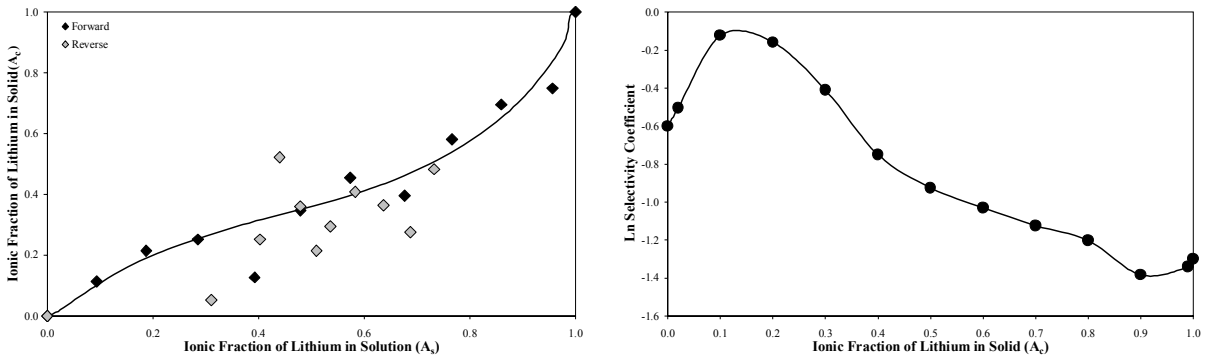

(a) **(b)**

Figure 1. (a) Li–Na isotherm; (b) Kielland plot of Li–Na on birnessite

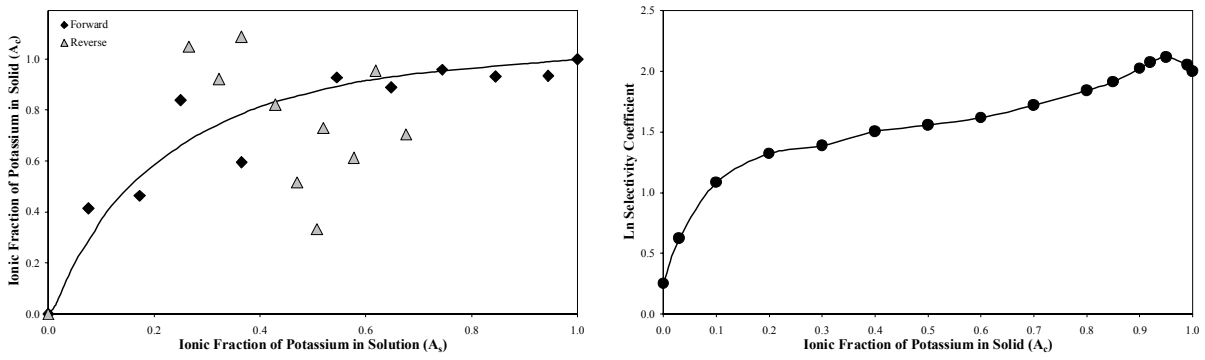

(a) **(b)**

Figure 2. (a) K–Na isotherm; (b) Kielland plot of K–Na on birnessite

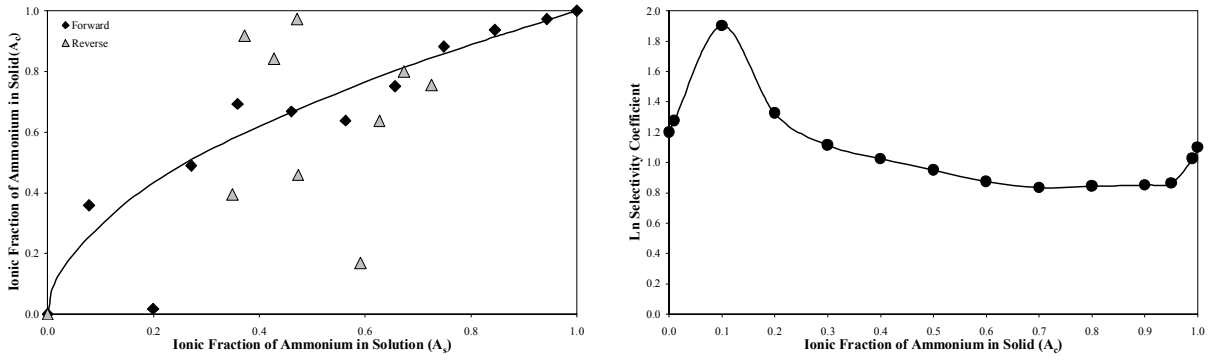

(a) **(b)**

Figure 3. (a) NH_4–Na isotherm; (b) Kielland plot of NH_4–Na on birnessite

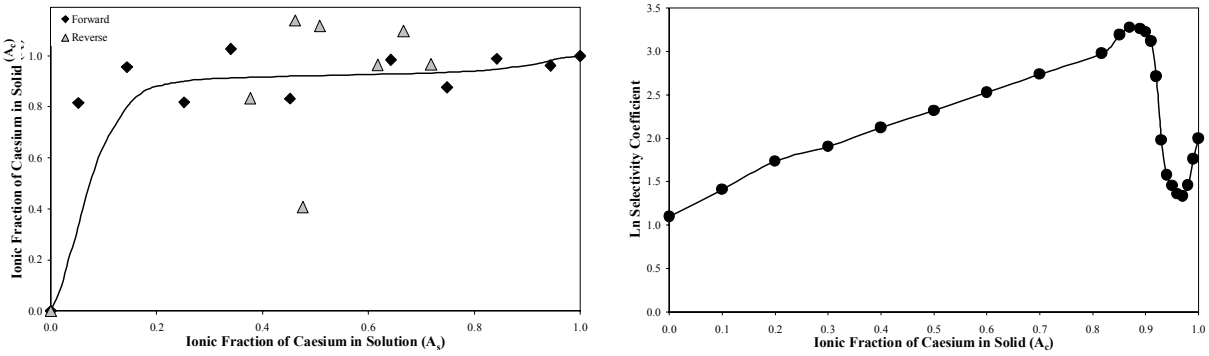

(a) **(b)**

Figure 4. (a) Cs–Na isotherm; (b) Kielland plot of Cs–Na on birnessite

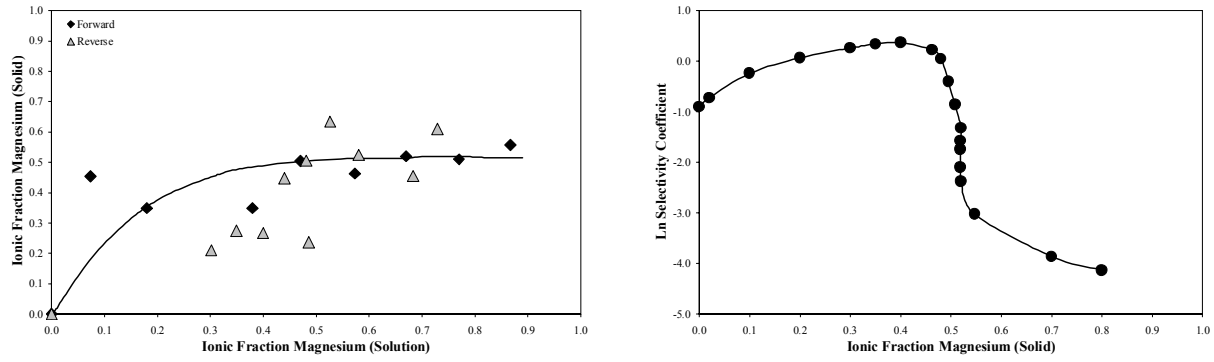

(a) **(b)**

Figure 5. (a) Mg–Na isotherm; (b) Kielland plot of Mg–Na on birnessite

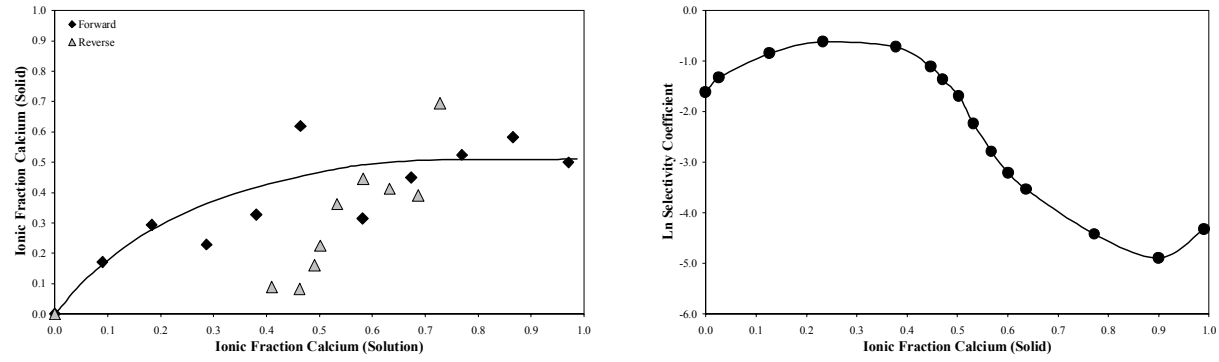

(a) **(b)**

Figure 6. (a) Ca–Na isotherm; (b) Kielland plot of Ca–Na on birnessite

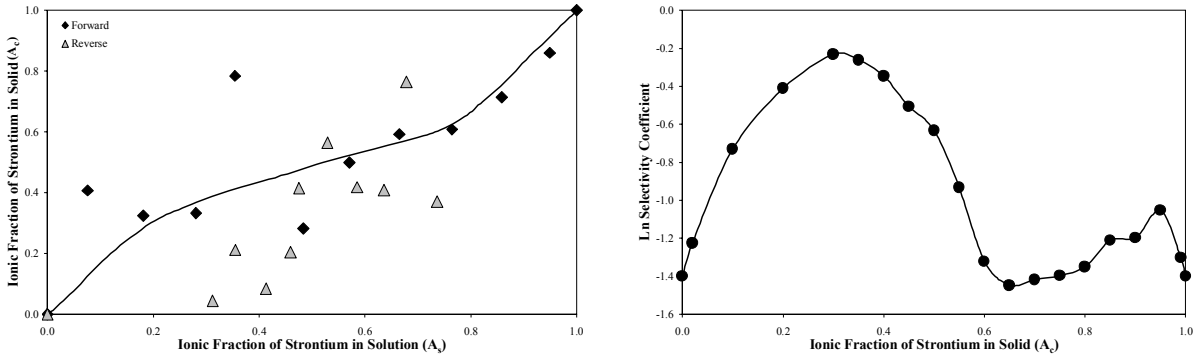

(a) (b)

Figure 7. (a) Sr–Na isotherm; (b) Kielland plot of Sr–Na on birnessite

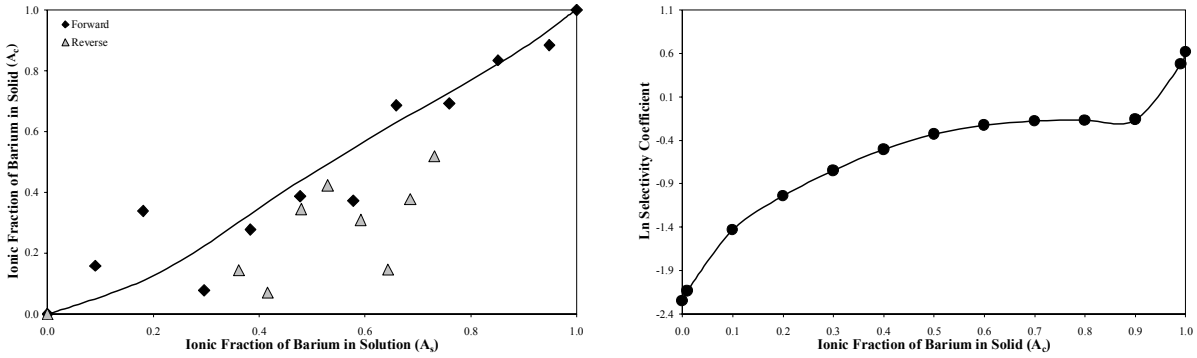

(a) (b)

Figure 8. (a) Ba–Na isotherm; (b) Kielland plot of Ba–Na on birnessite

3.4 Uni-divalent exchanges

Divalent exchange isotherms were predominantly 's' shaped (see Figures 5 to 7), with the exception of that for barium–sodium exchange – Figure 8. In the former cases, the isotherms showed that the selectivity of the material towards the in-going cation varied with the degree of exchange, whereas the barium–sodium system did not show any degree of selectivity. Its isotherm was close to the diagonal. The behaviour observed with divalent cations is a reflection of structural differences, as will now be considered.

The powder X-ray diffraction patterns agree well with those of the divalent exchanged-forms of birnessite prepared in previous work by these authors (Al-Attar and Dyer 2002). The Ca- and Mg-exchanged forms had their strongest peaks at *d*-spacings of 9.98 and 9.82 Å, respectively, and were assigned to the buserite structure. However, the Ba-exchanged form retained the birnessite structure, with a broad and less intense peak at a basal spacing of 7.12 Å. Thus, for divalent ions entering birnessite, it appeared that a significant ion sieving effect was taking place. According to Barrer and Klinowski (1972), the ion exchange capacity of an exchanger towards a particular cation is governed by three mechanisms, which account for an ion sieving effect:

(i) an exchanging cation may be too large to enter all sites, or access to some sites may be blocked by a locked-in cation resulting from a previous process;

(ii) the size of a hydrated exchanging cation, its energy of hydration and the consequent relative ease of co-ordinated water removal may

influence the degree of exchange;

(iii) charge distribution on the exchanger framework may not be favourable for a particular exchanging cation.

These factors can act singly or in unison. It can be concluded that factors (ii) and (iii) are the most likely to influence the divalent cation exchange in birnessite observed herein. Further discussion on this point will be considered in Sections 3.5 and 3.6.

3.5 Reversibility of ion exchange isotherms

All the systems examined, apart from Na/Cs, showed some degree of hysteresis when the forward arm was compared to that of the return.

Hysteresis is a well-known phenomenon in inorganic ion exchangers, and has been reviewed by Verburg and Baveye (1994). These authors emphasize the complex nature of this phenomenon, and cited the following possible mechanisms: (1) dehydration of the exchanger; (2) change in site heterogeneity at the surface; (3) differential hydration energy of cations; (4) inaccessibility of sites occupied by non-exchangeable cations.

In the work carried out here, dehydration of the exchanger can be excluded as an affecting factor, because wet samples were used to check reversibility. The heterogeneity of ion exchange sites is contributing in the case of the Na $\leftrightarrow$ ½ Mg/Ca exchanges, since these exchanges were associated with change from a birnessite to a buserite structure, bearing in mind that the buserite structure contains double water layers with an interlayer spacing of 10 Å. The Na/Mg and Na/Ca isotherms showed that approximately 50% of the available sites have been filled by the in-going cation. This was in contrast to the Na/Sr and Na/Ba isotherms which achieved complete replacement of the univalent cation. The XRD pattern of Ba confirms the retention of the birnessite structure. No XRD of the Sr birnessite was obtained.

It is worth mentioning that reverse experiments were performed at estimated solution–solid contact times. This might mean that the reverse step may have been kinetically controlled because full equilibrium had not been reached. In addition, since the reversibility tests were carried out on samples that had already been in the cation-exchanged form, it was possible that the cations introduced were occupying non-exchangeable sites.

3.6 Selectivity and thermodynamic approaches

A quantification of exchanger selectivity is provided by the values of free energy of exchange (ΔG^{θ}). The values of ΔG^{θ} are derived from a thermodynamic analysis of each ion exchange process. Strictly this should be fully reversible. Nevertheless, useful comparative data can be compiled from forward isotherms, as has been demonstrated for isotherms measured on clay minerals (Dyer *et al.*2000*c*).

Accordingly, Kielland plots were constructed, using the respective isotherm data for each forward exchange and the Kielland program provided on the University of Salford network. The plots are shown in Figures 1 (b) to 8 (b). Exchange constants and standard free energies for each forward exchange process were generated by the same program. The values acquired are given.

Table 2. Equilibrium constants, and estimated free energies for forward isotherms

Exchange system	Equilibrium constant $K_{(Na/M)}$	ΔG^{θ} (kJ/mol)
Li–Na	0.45	2.00
K–Na	4.64	–3.80
Cs–Na	8.43	–5.29
NH_4–Na	2.97	–2.69
Mg–Na	0.07	3.33
Ca–Na	0.03	6.16
Sr–Na	0.15	2.33
Ba–Na	0.21	1.94

Based on the standard free-energy values, the selectivity series in ^{22}Na-birnessite for univalent cations at 298 K is:

$$Cs^{+} > K^{+} \geq NH_4^{+} > Na^{+} > Li^{+} \qquad (1.2)$$

and for divalent cations it is:

$$Ba^{2+} > Sr^{2+} > Mg^{2+} > Ca^{2+} \qquad (1.3)$$

The univalent sequence follows the size of the hydrated ions, with caesium, the least hydrated cation,

being most preferred; and the smallest, highly hydrated, ions, such as lithium, being the least. Horvath (1985) states that hydrated ammonium and potassium ions are identical in size (3.31 Å), so the position of ammonium in the selectivity series was sensible.

The divalent selectivity series followed a similar sequence, apart from calcium. The material showed no preference for barium, the largest relatively unhydrated cation – Figure 8(a); there was a partial selectivity for the relatively highly hydrated cations up to a certain degree of exchange, after which the selectivity reversed (Figures 5 (a) to 7 (a)). Standard free energies were used comparatively because of their convenience. Theoretical analysis of ion exchange activity by Eisenman (1962) concluded that selectivity was controlled by the anionic field strength of the exchange site. For uni-univalent ion exchange, the reaction can be expressed as:

$$A_s^+ + B_z^+ = B_s^+ + A_z^+ \quad (1.4)$$

where A is the in-going cation, B is the out-going cation, and s and z represent the solution and exchanger phases, respectively.

The free energy of the reaction is considered to consist of two terms:

$$\Delta G^\theta = \left(G_Z^{\theta A+} - G_Z^{\theta B+}\right) - \left(G_S^{\theta A+} - G_S^{\theta B+}\right) \quad (1.5)$$

The first term represents the difference in the free energies of ions A^+ and B^+ in the exchanger, whereas the second term represents the difference in the free energies of the ions in solution, which equates to their free energy of hydration. The first term is more important when the field strength in the ion exchanger is very strong (e.g. zeolites with a high framework charge and correspondingly with a low silicon to aluminium ratio) and small ions are preferred. If the fields are weak (e.g. zeolites with a low framework change and correspondingly with a high silicon to aluminium ratio), the second term is more important, and large, weakly hydrated cations are preferred. Generally, the selectivity series constructed for univalent and divalent exchanges showed that the charge framework of the material was weak. This could be a result of the fact that, in the structure of birnessite, only one out of six sites in the octahedral manganese oxide layer is vacant, and that divalent and trivalent manganese ions are lying above and below the octahedral layer vacancies (Drits *et al.* 1997). Thus, the first term in equation 1.5 can be neglected. The second term depended upon the relative hydration energies of the cations in solution. The relationship of the standard free energy, hydration energy and entropy given by the following equation:

$$\Delta G = \Delta H - T\Delta S \quad (1.6)$$

The entropy term (ΔS) cannot be specified in this work, since exchange experiments were carried out at a fixed temperature, i.e. 298 K. Normally, transfer of water from solution to exchanger decreases with the increase in the atomic number of the univalent alkali metal ion present. This in turn decreases the entropy, because water molecules adsorbed in the exchanger will have less degree of freedom. In the case herein, the changes in layer structure during exchange may affect the entropy (ΔS) in a similar manner to that created by the release of waters of hydration from a cation in solution as it moves into the solid phase. However, if it could be assumed that ΔS has no effect, hence, the standard free energy of the reaction would only be related to the difference in the hydration energies. For the reasons mentioned, Equation (1.5) can be rewritten as follows:

$$\Delta G^\theta = H_S^{\theta B^+} - H_S^{\theta A^+} \quad (1.7)$$

This demonstrates how the change in hydration energies of the ions could affect the standard free energy of the ion exchange reaction.

It is well known that in inorganic exchangers the exchangeable cations may be present in different intracrystalline environments and this can result in cations sites which have different exchange properties. With reference to the exchange isotherms obtained in this study, it could be seen that the shape of virtually all divalent ion exchange isotherms arising from Na-birnessite (Figures 1(a) to 4(a)) would seem to indicate that only one type of exchange site was involved. The high (negative) free energy associated with caesium suggested that caesium was preferred to sodium, and to the divalent species. This arose from the ability of the large, weakly hydrated, caesium ion to occupy 'fixed' unhydrated positions in the birnessite structure, so that

the cation charge was unshielded from the negatively charged birnessite framework. The lithium isotherm was an exception related to the high hydration energy of lithium, as mentioned in Section 3.3. The occurrence of two sites, one of which was for univalent lithium cations, with the other for fully or partially hydrated Li species, may be possible. Feng *et al*. (1995), using pH titration, recorded the same selectivity order noted in this work for uptake of divalent cations on Na-birnessite. These authors inferred that univalent cations were located in site A, located on the crystal water sheet; whereas lithium was located in both sites, A and B, with site B located above and below the vacancies on the manganese oxide sheets.

It is also known that linear Kielland plots can be associated with single exchange sites; whereas more complex Kielland plots, for example those displaying the sigmoidal shape, were characteristic of crystallographically different exchange sites of different hydration energy (Barrer and Klinowski 1972), which was the case for the divalent cations examined in this work. The size correlation mirrored similar conclusions drawn from the relative sizes of the in-going and out-going cations involved in sodium–univalent exchanges. The results obtained in this study are unique, and no comparable data exist for divalent ion-sieve properties or isotherms of divalent-cation exchanges in birnessite. The use of forward isotherms only to generate thermodynamic data seems to have been justified, in that sensible comparisons have been seen. They reflected ion sizes, hydration energies, and structural changes in the material examined.

4 CONCLUSIONS

Studying the isotherms of ^{22}Na-birnessite exchanged by univalent and divalent cations gave a clear picture of the affinity of the material for a particular cation and the existing exchangeable sites. Sodium ions in birnessite were fully exchanged with univalent ions, apart from lithium, which was exchanged to a smaller extent because of its high hydration energy. Partial exchanges were seen with Ca and Mg cations. Reversible isotherms showed hysteresis resulting from variation in the hydration energies of the in-going and out-going cations and birnessite/buserite structural changes. Thermodynamic approaches drawn from these isotherms, as described in 3.5 and represented by their standard free energies, indicated that the selectivity of Na-birnessite was in the order of decreasing hydrated cation size. Of the divalent selectivity series, calcium exchange was an exception, since its framework reflected the occurrence of alternate single and double water layers.

Finally, birnessite minerals in soil can be expected to make significant contributions to the retention of those Cs and Sr radioisotopes that have entered the environment by accidental release or leakage from storage at nuclear sites, and to aid modelling associated with fission products in the ‘far-field’ environment of nuclear waste repositories.

ACKNOWLEDGEMENTS

L. Al-Attar acknowledges the Atomic Energy Commission of Syria for financial support throughout her work.

REFERENCES

Al-Attar, L. and Dyer, A. (2001) Sorption of uranium onto titanosilicate materials. *J. Radioanal. Nucl. Chem.*, **247**, 121

Al-Attar, L. and Dyer, A. (2002) Sorption behaviour of uranium on birnessite, a layered manganese oxide. *J. Mater. Chem.*, **12**, 1381

Al-Attar, L., Dyer, A. and Blackburn, R. (2000) Uptake of uranium on ETS-10 microporous titanosilicate. *J. Radioanal. Nucl. Chem*., **246**, 451

Al-Attar, L., Dyer, A., Harjula, R. and Paajanen, A. (2003*a*) Purification of nuclear wastes by novel inorganic ion exchangers. *J. Mater. Chem.*, **13**, 2969

Al-Attar, L., Dyer, A. and Harjula, R. (2003*b*) Uptake of radionuclides on microporous and layered ion exchange materials. *J. Mater. Chem.*, **13**, 2963

Al-Attar, L., Dyer, A. and Harjula, R. (2004) Uptake of radionuclides on antimony silicate. *J. Radioanal. Nucl. Chem.*, **260**, 199

Barrer, R.M. and Klinowski, J. (1972) Ion exchange involving several groups of homogeneous sites. *J. Chem. Soc., Faraday Trans. I*, **68**, 73

Bruno, J., Acros, D., Cera, E., Duro, L. and Grivé, M. (2004) Modelling near- and far-field processes in nuclear waste

management. *Geol. Soc., Special Publication*, **236** (1), 515. Geological Society, London

Committee on Radioactive Waste Management (UK) (CoRWM) (2006) *Managing Our Radioactive Waste Safely.* CORWM Doc 700

Drits, V.A., Silvester, E., Gorshkov, A.I. and Manceau, A. (1997) Structure of synthetic monoclinic Na-rich birnessite and hexagonal birnessite. 1. Results from X-ray diffraction and selected area electron diffraction. *Am. Mineral*., **82**, 946

Dyer, A. (2005) Ion-exchange in zeolites. *Stud. Surface Sci. Catalysis*, **157**, 181

Dyer, A., Pillinger, M., Harjula, R. and Amin, S. (2000*a*) Sorption characteristics of radionuclides on synthetic birnessite-type layered manganese oxides. *J. Mater. Chem.*, **10**, 1867

Dyer, A., Chow, J.K.K. and Umar, I.M. (2000*b*) The uptake of caesium and strontium onto clays. *J. Mater. Chem.*, **10**, 2734

Dyer, A., Pillinger, M., Newton, J., Harjula, R., Moller, T. and Amin, S. (2000*c*) Sorption behaviour of radionuclides on crystalline synthetic tunnel manganese oxides. *Chem. Mater.*, **12**, 3798

Eisenman, G. (1962) Cation selective glass electrodes and their mode of operation. *Biophys. J.*, **2**, 259

Feng, Q., Miyai, Y., Kanoh, H. and Ooi, K. (1992) Li extraction/insertion with spinel-type lithium manganese oxides, characterization of redox-type and ion-exchange type sites. *Langmiur*, **8**, 1861

Feng, Q., Kanoh, H., Miyai, Y. and Ooi, K. (1995) Metal-ion extraction/insertion reactions with todorokite-type manganese oxide in the aqueous phase. *Chem. Mater.*, **7**, 1226

Fletcher, P. and Townsend, R.P. (1982) Exchange of ammonium and sodium-ions in synthetic faujasites. *J. Chem. Soc., Faraday Trans. I*, **78**, 1741

Golden, D.C., Dixon, J.B. and Chen, C.C. (1986*a*) Ion exchange, thermal transformations and oxidising properties of birnessite. *Clays Clay Miner.*, **34**, 511

Golden, D.C., Chen, C.C. and Dixon, J.B. (1986*b*) Synthesis of todorokite. *Science*, **231**, 717

Golden, D.C., Chen, C.C. and Dixon, J.B. (1987) Transformation of birnessite to buserite, todorokite and manganite under mild hydrothermal treatment. *Clays Clay Miner.*, **35**, 271

Horvath, A.L. (1985) *Handbook of Aqueous Electrolyte Solutions*, p. 344. Ellis Horwood Ltd, New York

Jones, L.H.P. and Milne, A.A. (1956) Birnessite, a new manganese oxide from Aberdeenshire, Scotland. *Mineral. Mag.*, **31**, 283

McKenzie, R.M. (1970) Reaction of cobalt with manganese dioxide minerals. *Aust. J. Soil Res*., **8**, 97

Shen, Y.F., Zerger, R.P., De Guzman, R.N., Suib, S.L., McCurdy, L., Potter, D.I. and O'Young, C.L. (1993) Manganese octahedral molecular sieves – preparation, characterization and applications. *Science*, **260**, 511

Shen, Y.F., Suib, S.L. and O'Young, C.L. (1994) Effects of inorganic cation templates on octahedral molecular sieves of manganese oxide. *J. Am. Chem. Soc*., **116**, 11020–11029

Verburg, K. and Baveye, P. (1994) Hysteresis in the binary exchange of cations on 2/1 clay minerals – a critical review. *Clays Clay Miner.*, **42**, 207